Possible confirmation of the existence of the ergoregion by the Kerr quasinormal mode in gravitational waves from a Population III massive black hole binary

Kinugawa, Tomoya; Nakano, Hiroyuki; Nakamura, Takashi

PTEP

Prog. Theor. Exp. Phys. **2016**, 031E01 (9 pages)
DOI: 10.1093/ptep/ptw012

Letter

Possible confirmation of the existence of the ergoregion by the Kerr quasinormal mode in gravitational waves from a Population III massive black hole binary

Tomoya Kinugawa*, Hiroyuki Nakano, and Takashi Nakamura

Department of Physics, Kyoto University, Kyoto 606-8502, Japan
*E-mail: kinugawa@tap.scphys.kyoto-u.ac.jp

Received January 26, 2016; Accepted February 1, 2016; Published March 16, 2016

The existence of the ergoregion of the Kerr space-time has not yet been confirmed observationally. We show that the confirmation would be possible by observing the quasinormal mode in gravitational waves. As an example, using the recent population synthesis results of Population III (Pop III) binary black holes, we find that the peak of the final merger mass (M_f) is about $50\,M_\odot$, while the fraction of the final spin $q_f = a_f/M_f > 0.7$ needed for the confirmation of a part of the ergoregion is $\sim$77%. To confirm the frequency of the quasinormal mode, SNR > 35 is needed. The standard model of Pop III population synthesis tells us that the event rate for the confirmation of more than 50% of the ergoregion by second generation gravitational wave detectors is ~ 2.3 events yr^{-1} $(\mathrm{SFR_p}/(10^{-2.5}\,M_\odot\,\mathrm{yr}^{-1}\,\mathrm{Mpc}^{-3})) \cdot ([\mathrm{f_b}/(1+\mathrm{f_b})]/0.33)$, where $\mathrm{SFR_p}$ and $\mathrm{f_b}$ are the peak value of the Pop III star formation rate and the fraction of binaries, respectively.

Subject Index E01, E02, E31, E38

1. *Introduction* The Kerr space-time [1] is unique in two senses. First, it is the unique stationary solution [2–4] of the Einstein equation in the vacuum under cosmic censorship [5], which demands that the singularity should be covered by the event horizon. Secondly, it has the ergoregion where the time-like Killing vector turns out to be space-like. This causes various interesting mechanisms to extract the rotational energy of the Kerr black hole (BH) such as the Penrose process [5] and the Blanford–Znajek process [6]. Although there are many papers using these two mechanisms in the fields of physics and astrophysics, so far the existence of the ergoregion of the Kerr BH has not yet been confirmed observationally. In this paper, we suggest a possible method to confirm the existence of at least a part of the ergoregion.

The Kerr space-time in the geometric units of $G = c = 1$ is specified by its gravitational mass M and the specific angular momentum a. We use the non-dimensional spin parameter $q = a/M$ instead of a hereafter. There are two important quantities. The first is the outer event horizon radius r_+ defined by

$$r_+ = M\left(1 + \sqrt{1 - q^2}\right). \tag{1}$$

The second is the location of the outer boundary of the ergoregion ($r_{\rm ergo}(\theta)$) defined by

$$r_{\rm ergo}(\theta) = M\left(1+\sqrt{1-q^2\cos^2\theta}\right), \tag{2}$$

which is called the ergosphere. Note that $r_{\rm ergo}(0) = r_+$ and $r_{\rm ergo}(\pi/2) = 2M$.

The quasinormal mode (QNM) is the free oscillation of the Kerr BH after the merger of BH binaries. The complex QNM frequencies are determined by using Leaver's method [7] accurately. A recent numerical relativity simulation of a BH binary with initial equal masses and spins of $q_1 = q_2 = 0.994$ results in the final spin $q_f \sim 0.95$ [8]. As for the physical meaning of QNMs, Schutz and Will [9] used the Wentzel–Kramers–Brillouin (WKB) method for the $q_f = 0$ case, that is, the Schwarzschild space-time, and they showed that the real and imaginary parts of the QNMs are determined by the peak value and the second derivative, respectively, of the Regge–Wheeler potential [10], which determines the behavior of gravitational perturbations in the Schwarzschild space-time. The location of the peak for the dominant $\ell = 2$ mode is at $r_{\rm max} = 3.28$M, and the errors due to the WKB approximation are about 7% and 0.7% for the real and imaginary parts of the fundamental ($n = 0$) QNM frequency, respectively. This suggests that the complex frequency of the QNM is determined by the space-time around $r_{\rm max}$. Conversely, if the $\ell = 2$ QNM, which is the dominant mode, is confirmed by the second generation gravitational wave detectors, such as Advanced LIGO (aLIGO) [11], Advanced Virgo (AdV) [12], and KAGRA [13,14], we can say that the strong space-time around $r = 3.28$M is confirmed as predicted by Einstein's general relativity. The reason for the word "around" comes from the fact that the imaginary part of the QNM frequency is determined by the second derivative of the Regge–Wheeler potential.

Nakano, Nakamura, and Tanaka [15] showed that a similar physical picture to that presented by Schutz and Will can be obtained by using the Detweiler potential [16] of gravitational perturbations [17] in the Kerr space-time.[1] The maximum errors of the real and imaginary parts of the QNM frequency with ($\ell = m = 2$), which is the dominant mode shown by the numerical relativity simulations [20], are $\lesssim$1.5% and $\lesssim$2%, respectively, in the range of $0.7 < q_f < 0.98$. They also found that the QNM for $q_f > 0.7$ reflects the Kerr space-time within the ergoregion because $r_{\rm max} < 2$M. Since the ergoregion radius depends on θ, we can define the covered solid angle $4\pi C$ for each $r_{\rm max} < 2$M by $C = \cos\theta_m$, with θ_m defined by $r_{\rm max} = M(1+\sqrt{1-q^2\cos^2\theta_m})$. It is found that an empirical relation between $(1-C)$ and $(1-q)$ for $0.7 < q < 0.98$ exists, and is given by

$$\ln(1-C) = 2.7867\ln(1-q) + 3.0479. \tag{3}$$

The correlation coefficient of this empirical relation is 0.989, with the chance probability of 5.9×10^{-8}.

The purpose of this paper is to apply Eq. (3) to the recent population synthesis results of Population III (Pop III) massive BH binaries to find the event rate of detection of the QNM gravitational waves and the typical value of C as an example.

This paper is organized as follows. In Sect. 2, we briefly describe the recent population synthesis results of Pop III massive BH binaries [21,22]. The reader who is not familiar with the population synthesis may skip this section. In Sect. 3, we discuss methods to obtain the final BH's mass M_f and

[1] Note that the Detweiler potential corresponds to either the Regge–Wheeler or Zerilli [18] potential in the Schwarzschild space-time (see also Ref. [19]).

spin q_f with their distribution functions and the detection rate as a function of C. Finally, Sect. 4 is devoted to discussion.

2. *Population III binary calculation* A Pop III star is the first star in our universe which does not have metal with atomic number larger than carbon. To study Pop III binary evolutions, a Pop III binary population synthesis code was used [21,22] which is upgraded from Hurley's BSE code [23][2] for the case of Pop I stars to that of Pop III stars. They calculated 10^6 binary evolutions for given initial values of the primary mass M_1, the mass ratio M_2/M_1, the orbital separation a, and the eccentricity e using the Monte Carlo method under the initial distribution functions. They call the star with the larger mass the primary, while the secondary is the star with the smaller mass. The typical mass of Pop III stars is from $\sim 10\,\mathrm{M}_\odot$ to $\sim 100\,\mathrm{M}_\odot$ [24,25]. Thus, they took an initial mass function which may be flat from $10\,\mathrm{M}_\odot$ to $140\,\mathrm{M}_\odot$ as suggested by the numerical simulations [26,27]. The reason for the upper limit of mass of $140\,\mathrm{M}_\odot$ is that a star with mass larger than $140\,\mathrm{M}_\odot$ causes a pair-instability supernova, leaving no remnant. Since there is no observation of Pop III stars and binaries, they simply assume that other initial distribution functions are the same as Pop I binaries. The initial mass ratio function for given M_1 is flat from $10\,\mathrm{M}_\odot/M_1$ to 1. The separation (a)[3] distribution function is proportional to $1/a$ from $a_{\min}$ to $10^6\,\mathrm{R}_\odot$, where $a_{\min}$ is the minimum separation when binary interaction such as mass transfer is absent. The initial eccentricity distribution function is proportional to e from 0 to 1. The set of these initial distribution functions is the same as their standard model with the 140 case of Ref. [22]. In this paper, we choose the binary evolution parameters of their standard model and the optimistic core-merger criterion of Ref. [22]. The details of binary interactions and spin evolution, which are very important in this paper, are discussed in Refs. [21,22].

In Ref. [22], they found that $\sim 13\,\%$ of Pop III binaries become BH–BH binaries which merge within the Hubble time, and the typical mass of Pop III BHs is $\sim 30\,\mathrm{M}_\odot$. Figure 1 shows the initial mass ratio distribution of Pop III binaries (red line) and that of Pop III BH–BHs (blue dashed line). Even though the mass ratio of binaries smaller than ~ 0.5 is initially substantial, most of the BH–BH binaries have mass ratio larger than ~ 0.5 by the effect of mass transfer. Thus, large mass ratio $(=M_2/M_1)$ BH–BHs are the majority.

Figure 2 shows the distribution of spin parameters of the primary and secondary BHs when the primary and secondary become BHs. Figure 3 shows cross-section views of the distribution of the spin parameter with (a) cross-section views of the distribution of the spin parameter when $0 < q_1 < 0.05$, and (b) cross-section views of the distribution of the spin parameter when $0.95 < q_1 < 0.998$. The spin parameter of each BH is calculated by the angular momentum of the progenitor just before it becomes a BH. If the spin parameter of the BH is larger than the Thorne limit [28], we assign $q = q_{\mathrm{Thorne}} = 0.998$ as the spin parameter. From Figs. 2 and 3, the spin parameters of Pop III BH–BHs are roughly classified into three groups. First, the majority of Pop III is in the group where both BHs have high spin parameters. If the mass transfer is dynamically unstable or the secondary plunges into the primary envelope, the orbit shrinks and the primary envelope is stripped by the friction between the secondary and the primary envelope [29]. In this group, the progenitors evolve without the common envelope phase and the primary envelope is not stripped. Thus, BHs of this group get large angular momentum from the envelope of the progenitor and the spin parameter which

[2] http://astronomy.swin.edu.au/~jhurley/.
[3] This "a" is completely different from the "a" in the Kerr BH, so we use $q = a/M$ as the Kerr parameter.

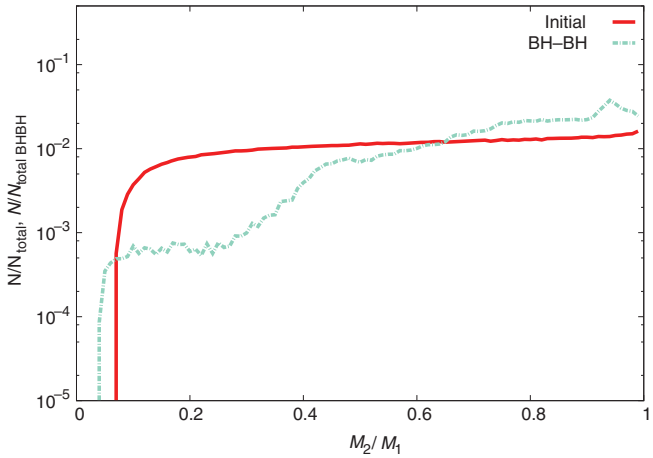

Fig. 1. The distribution of mass ratio $M_2/M_1 \leq 1$. The distributions of the initial mass ratio and when the binaries become BH–BHs are shown as red and light blue lines, respectively. The initial mass ratio distribution is normalized by the total binary number $N_{\rm total} = 10^6$, while that when the binaries become BH–BHs is normalized by the total binary number $N_{\rm total\,BHBH} = 128897$.

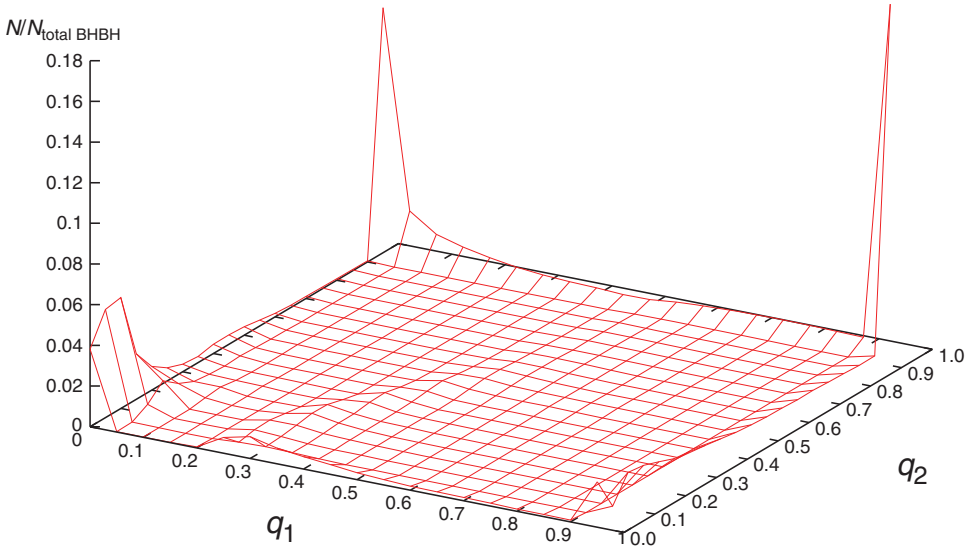

Fig. 2. The distribution of spin parameters. The distribution of spin parameters when each star becomes a BH is shown. q_1 and q_2 are the spin parameters of the primary and the secondary BHs, respectively. The distribution when the binaries become BH–BHs is normalized by the total binary number $N_{\rm total\,BHBH} = 128897$, with the grid separation being $\Delta q_1 = \Delta q_2 = 0.05$.

has the largest Thorne limit $q_{\rm Thorne} = 0.998$. Second, there is a group where both BHs have low spin parameters. In this group, each star evolves via the common envelope phase and then they leave their envelope and lose almost all of the angular momentum. Thus, there are many Pop III BH–BHs with $q_1 < 0.15$, $q_2 < 0.15$. Third, there is a group where one of the pair has high spin and the other has low spin. In this group, the primary evolves with the common envelope phase and the secondary evolves without the common envelope, or vice versa.

3. *Remnant mass, spin, and the detection rate* Given BH binary parameters M_1, M_2, q_1, and q_2, we calculate the remnant mass and spin by using formulae from spin-aligned BH binaries [30,31] (see also Refs. [32,33] from a different group).

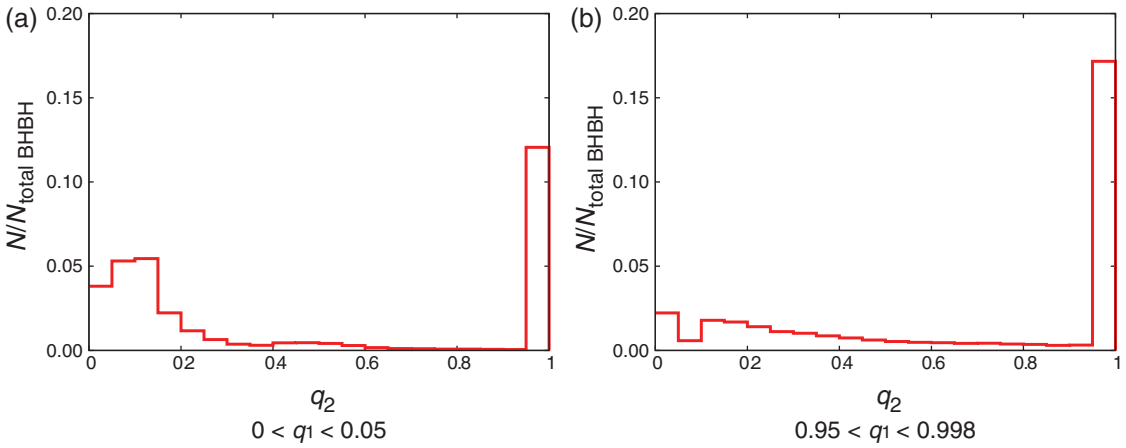

Fig. 3. Cross-section views of the spin parameter distribution. (a) The distribution of q_2 for $0 < q_1 < 0.05$. We can see that the q_2 distribution has bimodal peaks at $0 < q_2 < 0.15$ and $0.95 < q_2 < 0.998$. (b) The distribution of q_2 for $0.95 < q_1 < 0.998$. We see that the large value of q_2 is the majority so that there is a group in which both q_1 and q_2 are large.

The final (non-dimensional) spin parameter q_f is

$$q_f = \frac{S_f}{M_f^2} = (4\eta)^2 \left(L_0 + L_1 \tilde{S}_\parallel + L_{2a} \tilde{\Delta}_\parallel \delta m + \cdots\right) + (1 + 8\eta)\tilde{S}_\parallel \delta m^4 + \eta \tilde{J}_{\rm ISCO} \delta m^6, \quad (4)$$

where

$$\eta = \frac{M_1 M_2}{M^2}, \quad M = M_1 + M_2, \quad \delta m = \frac{M_1 - M_2}{M},$$
$$\tilde{S}_\parallel = \frac{M_1^2 q_1 + M_2^2 q_2}{M^2}, \quad \tilde{\Delta}_\parallel = \frac{M_2 q_2 - M_1 q_1}{M}, \quad (5)$$

and $(+\cdots)$ denotes the higher-order correction with respect to spins which is given explicitly in Eq. (14) of Ref. [31]. L_0, L_1, and L_{2a} are the fitting parameters summarized in Table VI of Ref. [31], and the last two terms in Eq. (4) are added to enforce the particle limit ($\eta \to 0$) where $\tilde{J}_{\rm ISCO}$ is the orbital angular momentum of the innermost stable circular orbit (ISCO). The final mass M_f is given by

$$\frac{M_f}{M} = (4\eta)^2 \left(M_0 + K_1 \tilde{S}_\parallel + K_{2a} \tilde{\Delta}_\parallel \delta m + \cdots\right) + \left[1 + \eta \left(\tilde{E}_{\rm ISCO} + 11\right)\right] \delta m^6. \quad (6)$$

Again, M_0, K_1, and K_{2a} are the fitting parameters summarized in Table VI of Ref. [31]. In practice, we use Ref. [34] for the ISCO angular momentum and energy, $\tilde{J}_{\rm ISCO}$ and $\tilde{E}_{\rm ISCO}$ (note that we assign q_f to a in Ref. [34]).

According to a recent numerical relativity simulation for a highly spinning BH binary merger with $M_1 = M_2 = 1/2$, $q_1 = q_2 = 0.994$ [8], the final mass and spin after merger are obtained as $M_{\rm f} = 0.887$ and $q_{\rm f} = 0.950$, respectively. On the other hand, the remnant formulae in Eqs. (4) and (6), which are not calibrated by the above numerical relativity result, give $M_f = 0.888$ and $q_f = 0.950$. We see that the formulae are sufficiently accurate for our analysis (see also a recent study on remnant BHs for precessing BH binaries [35]). The radiated energy is so large that the total mass of $60\,{\rm M}_\odot$ for the above highly spinning binaries becomes the remnant mass of $53.28\,{\rm M}_\odot$. We note that Eq. (4) cannot give any realistic solution for some large mass ratios, e.g., for $\eta \gtrsim 0.1249$ ($q_1 = q_2 = 0.998$), $\eta \gtrsim 0.1169$ ($q_1 = q_2 = 0.994$), and $\eta \gtrsim 0.1066$ ($q_1 = q_2 = 0.99$). In that case, we simply set $q_f = 0.998$.

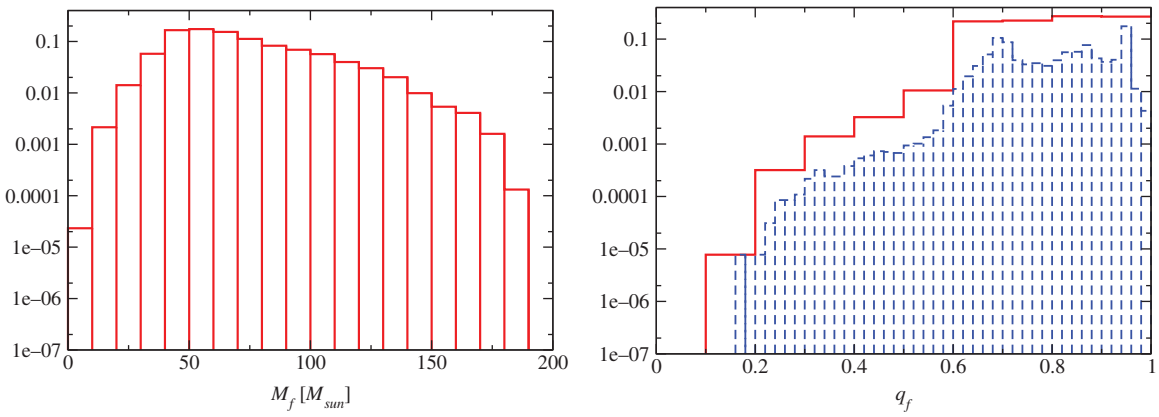

Fig. 4. (Left) The normalized distribution of M_f obtained by binning with $\Delta M_f = 10\,\mathrm{M}_\odot$. (Right) The normalized distribution of q_f. The solid red and dashed blue lines are obtained by binning with $\Delta q_f = 0.1$ and 0.02, respectively.

In Fig. 4, we show the remnant mass and spin calculated by the remnant formulae. Due to the mass decrease by gravitational wave radiation, we see a peak in a bin between $50\,\mathrm{M}_\odot$ and $60\,\mathrm{M}_\odot$, which reflects the peak of the total mass of Pop III BH–BHs. The remnant spin $q_f > 0.96$ is 1.56%, and only 0.429% of the remnant BHs have spin larger than 0.98.

To estimate the signal-to-noise ratio (SNR) of the QNM (ringdown) signal in the expected noise curve of KAGRA [13,14] (bKAGRA, VRSE(D) configuration),[4] we use the results derived by Flanagan and Hughes in Ref. [36]. In Ref. [37], we have fitted the KAGRA noise curve as

$$S_n(f)^{1/2} = 10^{-26}\left(6.5\times10^{10} f^{-8} + 6\times10^{6} f^{-2.3} + 1.5 f^{1}\right)\left[\mathrm{Hz}^{-1/2}\right], \tag{7}$$

where the frequency f is in units of Hz. According to Ref. [36], the angle-averaged SNR for the ringdown phase is calculated from Eq. (B14) of Ref. [36] as

$$\mathrm{SNR} = \sqrt{\frac{128}{5}}\frac{\eta}{F(q_f)}\sqrt{\frac{\epsilon_r M_f}{S_n(f_c)}}\frac{M_f}{D}, \tag{8}$$

where $F(q_f)$ and f_c are given in Ref. [38],

$$F(q_f) = 1.5251 - 1.1568(1-q_f)^{0.1292}, \quad f_c = \frac{1}{2\pi M_f}F(q_f), \tag{9}$$

and ϵ_r denotes the fraction of the total mass energy radiated in the ringdown phase, which is assumed to be $\epsilon_r = 0.03$. Here, we have ignored effects of the redshifted mass and the cosmological distance, i.e., the redshift and the difference between the distance D and the luminosity distance. Since the maximum distance considered here is $z \sim 0.28$, the errors are small. Although the calculation is straightforward, we do not show the explicit expression since the expression is complicated due to $S_n(f_c)$. For example, we have SNR = 23 in the case of $M_f = 60\,\mathrm{M}_\odot$, $q_f = 0.7$, $\eta = 1/4$, and $D = 200\,\mathrm{Mpc}$.

Figure 5 shows the normalized distribution of the SNRs. Here, we have assumed all gravitational wave sources are located at $D = 200\,\mathrm{Mpc}$. To calculate the detection rate, we need to know the merger rate density of Pop III BH–BHs. The merger rate density derived in Ref. [22] is approximated

[4] See http://gwcenter.icrr.u-tokyo.ac.jp/researcher/parameters.

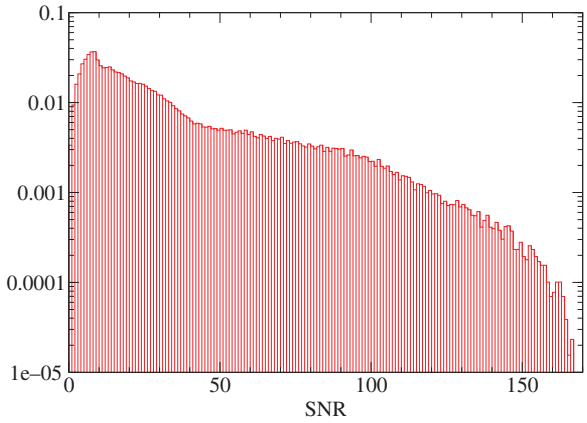

Fig. 5. The normalized distribution of SNRs obtained by binning with $\Delta\mathrm{SNR} = 1$, calculated from Eq. (8) for $D = 200\,\mathrm{Mpc}$.

Table 1. The detection rate [yr^{-1}] divided by dependence on the star formation rate $\mathrm{SFR_p}$ and the fraction of the binary $\mathrm{f_b}$ as a function of the lower limit of the solid angle of the sphere $4\pi C$ where the QNM is mainly emitted from the ergoregion in the case of $\mathrm{SNR} = 35$ for the KAGRA detector.

$0 < C$	$0.5 < C$	$0.7 < C$	$0.9 < C$	$0.95 < C$	$0.97 < C$	$0.99 < C$
3.73	2.23	1.10	0.356	0.162	0.117	0.0780

by $R_m = 0.024 + 0.0080\,(D/1\,\mathrm{Gpc})\,[\mathrm{Myr}^{-1}\,\mathrm{Mpc}^{-3}]$ for a low redshift (note that this fit works up to $z \sim 2$).

In this paper, we focus on the detection rate of the solid angle of a sphere emitting the QNM, $4\pi C$ which dips in the ergoregion. In Nakano, Nakamura and Tanaka's paper [15], we obtained a simple relation between C and the spin parameter q, shown as Eq. (3) in Sect. 1. In Table 1, we present the result for the detection rate in the case of $\mathrm{SNR} = 35$, which is needed to confirm the QNM [39].

4. *Discussion* In this paper, we have taken only BH–BH binaries from Pop III star origin as an example. In Table 1, the standard model of Pop III population synthesis [21,22] tells us that the event rate for the confirmation of more than 50% of the ergoregion by second generation gravitational wave detectors is $\sim$2.3 events yr^{-1} $(\mathrm{SFR_p}/(10^{-2.5}\,\mathrm{M_\odot\,yr^{-1}\,Mpc^{-3}})) \cdot ([\mathrm{f_b}/(1+\mathrm{f_b})]/0.33)$, where $\mathrm{SFR_p}$ and $\mathrm{f_b}$ are the peak value of the Pop III star formation rate and the fraction of binaries, respectively. Here, we set $\mathrm{SNR} = 35$ because at least this SNR is needed to confirm the QNM frequency. Furthermore, by massive Pop I and Pop II binaries, the above rate could get larger. Here, Pop I stars are Sun-like ones with $\sim$2% metal in their weight, while Pop II are old stars like those in the globular cluster with $\sim 10^{-2}$% metal. The Pop I and Pop II binary population synthesis [40–42] showed that the some fraction of Pop II evolves into massive BH–BHs. In addition, rotating Pop II stars become massive BH-BHs more easily than non-rotating Pop II stars [43,44]. Since mass loss is expected for Pop I and Pop II stars due to the absorption of photons at the spectral lines of metals, these Pop I and Pop II progenitors more easily lose angular momentum by stellar wind mass loss and so on. Thus, the Pop I and Pop II cases might have lower spin than the Pop III case. If, however, the mass and spin distributions of Refs. [42–44] are available, we can compute the detection rate of the QNM and the covered solid angle $4\pi C$ of the ergoregion. In this sense, the rate shown in this paper is the minimum.

It is noted that from the standard model of Pop III population synthesis, the event rate of the final $q_f > 0.98$ BHs is $\sim 5.17 \times 10^{-6}$ events yr^{-1} $(\mathrm{SFR_p}/(10^{-2.5}\,\mathrm{M_\odot\,yr^{-1}\,Mpc^{-3}})) \cdot ([\mathrm{f_b}/(1+\mathrm{f_b})]/0.33)$ for SNR $= 35$. We expect interesting physics in highly/extremely spinning Kerr BHs, which needs further studies. To detect such a BH, third generation gravitational wave detectors, such as the Einstein Telescope (ET) [45], should be required. Also, although there is room for highly spinning remnant BHs with $q_f > 0.98$ from the merger of comparable mass BH binaries, we will need large-mass-ratio binaries for which the cosmic censorship [5] has been discussed extensively (see, e.g., Ref. [46] and references therein). These binaries could be one of the targets for space-based gravitational wave detectors such as eLISA [47] and DECIGO [48] at the formation time of $z \sim 10$.

Acknowledgements

This work was supported by MEXT Grant-in-Aid for Scientific Research on Innovative Areas, "New Developments in Astrophysics Through Multi-Messenger Observations of Gravitational Wave Sources," No. 24103006 (TN, HN) and by Grants-in-Aid from the Ministry of Education, Culture, Sports, Science and Technology (MEXT) of Japan Nos. 251284 (TK) and 15H02087 (TN).

References

[1] R. P. Kerr, Phys. Rev. Lett. **11**, 237 (1963).
[2] W. Israel, Phys. Rev. **164**, 1776 (1967).
[3] B. Carter, Phys. Rev. Lett. **26**, 331 (1971).
[4] D. C. Robinson, Phys. Rev. Lett. **34**, 905 (1975).
[5] R. Penrose, Riv. Nuovo Cim. **1**, 252 (1969) [Gen. Rel. Grav. **34**, 1141 (2002)].
[6] R. D. Blandford and R. L. Znajek, Mon. Not. Roy. Astron. Soc. **179**, 433 (1977).
[7] E. W. Leaver, Proc. Roy. Soc. Lond. A **402**, 285 (1985).
[8] M. A. Scheel, M. Giesler, D. A. Hemberger, G. Lovelace, K. Kuper, M. Boyle, B. Szilagyi, and L. E. Kidder, Class. Quant. Grav. **32**, 105009 (2015) [arXiv:1412.1803 [gr-qc]] [Search INSPIRE].
[9] B. F. Schutz and C. M. Will, Astrophys. J. **291**, L33 (1985).
[10] T. Regge and J. A. Wheeler, Phys. Rev. **108**, 1063 (1957).
[11] J. Aasi et al. [LIGO Scientific Collaboration], Class. Quant. Grav. **32**, 074001 (2015) [arXiv:1411.4547 [gr-qc]] [Search INSPIRE].
[12] F. Acernese et al. [VIRGO Collaboration], Class. Quant. Grav. **32**, 024001 (2015) [arXiv:1408.3978 [gr-qc]] [Search INSPIRE].
[13] K. Somiya [KAGRA Collaboration], Class. Quant. Grav. **29**, 124007 (2012) [arXiv:1111.7185 [gr-qc]] [Search INSPIRE].
[14] Y. Aso et al. [KAGRA Collaboration], Phys. Rev. D **88**, 043007 (2013) [arXiv:1306.6747 [gr-qc]] [Search INSPIRE].
[15] H. Nakano, T. Nakamura, and T. Tanaka, [arXiv:1602.02875 [gr-qc]] [Search INSPIRE].
[16] S. L. Detweiler, Proc. Roy. Soc. Lond A **352**, 381 (1977).
[17] S. A. Teukolsky, Astrophys. J. **185**, 635 (1973).
[18] F. J. Zerilli, Phys. Rev. D **2**, 2141 (1970).
[19] T. Nakamura, H. Nakano, and T. Tanaka, [arXiv:1601.00356 [astro-ph.HE]] [Search INSPIRE].
[20] L. London, D. Shoemaker, and J. Healy, Phys. Rev. D **90**, 124032 (2014) [arXiv:1404.3197 [gr-qc]] [Search INSPIRE].
[21] T. Kinugawa, K. Inayoshi, K. Hotokezaka, D. Nakauchi, and T. Nakamura, Mon. Not. Roy. Astron. Soc. **442**, 2963 (2014) [arXiv:1402.6672 [astro-ph.HE]] [Search INSPIRE].
[22] T. Kinugawa, A. Miyamoto, N. Kanda, and T. Nakamura, [arXiv:1505.06962 [astro-ph.SR]] [Search INSPIRE].
[23] J. R. Hurley, C. A. Tout, and O. R. Pols, Mon. Not. Roy. Astron. Soc. **329**, 897 (2002) [arXiv:astro-ph/0201220] [Search INSPIRE].
[24] T. Hosokawa, K. Omukai, N. Yoshida, and H. W. Yorke, Science **334**, 1250 (2011) [arXiv:1111.3649 [astro-ph.CO]] [Search INSPIRE].

[25] T. Hosokawa, N. Yoshida, K. Omukai, and H. W. Yorke, Astrophys. J. **760**, L37 (2012) [arXiv:1210.3035 [astro-ph.CO]] [Search INSPIRE].
[26] S. Hirano, T. Hosokawa, N. Yoshida, H. Umeda, K. Omukai, G. Chiaki, and H. W. Yorke, Astrophys. J. **781**, 60 (2014) [arXiv:1308.4456 [astro-ph.CO]] [Search INSPIRE].
[27] H. Susa, K. Hasegawa, and N. Tominaga, Astrophys. J. **792**, 32 (2014) [arXiv:1407.1374 [astro-ph.GA]] [Search INSPIRE].
[28] K. S. Thorne, Astrophys. J. **191**, 507 (1974).
[29] R. F. Webbink, Astrophys. J. **277**, 355 (1984).
[30] C. O. Lousto, M. Campanelli, Y. Zlochower, and H. Nakano, Class. Quant. Grav. **27**, 114006 (2010) [arXiv:0904.3541 [gr-qc]] [Search INSPIRE].
[31] J. Healy, C. O. Lousto, and Y. Zlochower, Phys. Rev. D **90**, 104004 (2014) [arXiv:1406.7295 [gr-qc]] [Search INSPIRE].
[32] E. Barausse and L. Rezzolla, Astrophys. J. **704**, L40 (2009) [arXiv:0904.2577 [gr-qc]] [Search INSPIRE].
[33] E. Barausse, V. Morozova, and L. Rezzolla, Astrophys. J. **758**, 63 (2012); **786**, 76 (2014) [erratum] [arXiv:1206.3803 [gr-qc]] [Search INSPIRE].
[34] A. Ori and K. S. Thorne, Phys. Rev. D **62**, 124022 (2000) [arXiv:gr-qc/0003032] [Search INSPIRE].
[35] Y. Zlochower and C. O. Lousto, Phys. Rev. D **92**, 024022 (2015) [arXiv:1503.07536 [gr-qc]] [Search INSPIRE].
[36] E. E. Flanagan and S. A. Hughes, Phys. Rev. D **57**, 4535 (1998) [arXiv:gr-qc/9701039] [Search INSPIRE].
[37] H. Nakano, T. Tanaka, and T. Nakamura, Phys. Rev. D **92**, 064003 (2015) [arXiv:1506.00560 [astro-ph.HE]] [Search INSPIRE].
[38] E. Berti, V. Cardoso, and C. M. Will, Phys. Rev. D **73**, 064030 (2006) [arXiv:gr-qc/0512160] [Search INSPIRE].
[39] E. Berti, J. Cardoso, V. Cardoso, and M. Cavaglia, Phys. Rev. D **76**, 104044 (2007) [arXiv:0707.1202 [gr-qc]] [Search INSPIRE].
[40] M. Dominik, K. Belczynski, C. Fryer, D. E. Holz, E. Berti, T. Bulik, I. Mandel, and R. O'Shaughnessy, Astrophys. J. **759**, 52 (2012) [arXiv:1202.4901 [astro-ph.HE]] [Search INSPIRE].
[41] M. Dominik, K. Belczynski, C. Fryer, D. E. Holz, E. Berti, T. Bulik, I. Mandel, and R. O'Shaughnessy, Astrophys. J. **779**, 72 (2013) [arXiv:1308.1546 [astro-ph.HE]] [Search INSPIRE].
[42] M. Dominik et al., Astrophys. J. **806**, 263 (2015) [arXiv:1405.7016 [astro-ph.HE]] [Search INSPIRE].
[43] I. Mandel and S. E. de Mink, [arXiv:1601.00007 [astro-ph.HE]] [Search INSPIRE].
[44] P. Marchant, N. Langer, P. Podsiadlowski, T. Tauris, and T. Moriya, [arXiv:1601.03718 [astro-ph.SR]] [Search INSPIRE].
[45] M. Punturo et al., Class. Quant. Grav. **27**, 194002 (2010).
[46] E. Barausse, V. Cardoso, and G. Khanna, Phys. Rev. D **84**, 104006 (2011) [arXiv:1106.1692 [gr-qc]] [Search INSPIRE].
[47] P. A. Seoane et al. [eLISA Collaboration], [arXiv:1305.5720 [astro-ph.CO]] [Search INSPIRE].
[48] N. Seto, S. Kawamura, and T. Nakamura, Phys. Rev. Lett. **87**, 221103 (2001) [arXiv:astro-ph/0108011] [Search INSPIRE].